Neoplastic and Non-neoplastic Proliferative Disorders of the Perirenal Space: Cross-sectional Imaging Findings[1]

Venkateswar R. Surabhi, MD[2] • Christine Menias, MD • Srinivasa R. Prasad, MD • Ankitkumar H. Patel, MD • Arpit Nagar, MD • Neal C. Dalrymple, MD

CME FEATURE

See accompanying test at http://www.rsna.org/education/rg_cme.html

LEARNING OBJECTIVES FOR TEST 2

After reading this article and taking the test, the reader will be able to:

- Describe the spectrum of neoplastic and nonneoplastic proliferative conditions that may involve the perirenal space.
- Identify the imaging features of perirenal tumors and pseudotumors and correlate them with histopathologic findings.
- Define a pattern-based approach to diagnostic imaging of perirenal tumors and pseudotumors.

TEACHING POINTS

See last page

The perirenal space, located between the anterior and the posterior renal fasciae, is shaped like an inverted cone with an apex that extends into the iliac fossa. Perirenal tumors and pseudotumors primarily originate either from the kidney or as part of a systemic disease process and have characteristic histopathologic features and biologic behavior. The lesions may be classified on the basis of their distribution and imaging features as solitary soft-tissue masses (renal cell carcinoma, lymphangioma, hemangioma, and leiomyoma), rindlike soft-tissue lesions (lymphoma, retroperitoneal fibrosis, and Erdheim-Chester disease), masses containing macroscopic fat (angiomyolipoma, liposarcoma, myelolipoma, and extramedullary hematopoiesis), and multifocal soft-tissue masses (metastases, plasma cell tumors). Because of overlap in imaging findings among these diverse perirenal lesions, a definitive diagnosis in most cases can be established only at histopathologic analysis. However, an imaging pattern–based approach may facilitate the diagnosis and optimal management of perirenal tumors and pseudotumors.

Abbreviation: GIST = gastrointestinal stromal tumor

RadioGraphics 2008; 28:1005–1017 • **Published online** 10.1148/rg.284075157 • **Content Codes:** GU OI

[1]From the Department of Radiology, University of Texas Health Science Center at San Antonio, 7703 Floyd Curl Dr, San Antonio, TX 78229 (V.R.S., S.R.P., A.H.P., A.N., N.C.D.); and Mallinckrodt Institute of Radiology, Washington University School of Medicine, St. Louis, Mo (C.M.). Presented as an education exhibit at the 2006 RSNA Annual Meeting. Received July 11, 2007; revision requested September 11, 2007, and received January 4, 2008; accepted January 30. All authors have no financial relationships to disclose. **Address correspondence to** S.R.P. (e-mail: *prasads@uthscsa.edu*).

[2]**Current address:** Department of Diagnostic and Interventional Imaging at the University of Texas Health Science Center, Houston, Texas.

Introduction

The perirenal space is a retroperitoneal space that is limited anteriorly by the anterior renal fascia (Gerota fascia) and posteriorly by the posterior renal fascia (Zuckerkandl fascia). These two fasciae fuse to form the lateroconal fascia laterally and blend loosely with the periureteric connective tissue medially (1,2). Superiorly, the two fasciae are fixed to the diaphragmatic fascia above the adrenal glands; inferiorly, they blend with the iliac fascia. The anterior and posterior renal fasciae enclose a gradually tapering conelike space produced by the embryologic ascent of the kidneys from the pelvis to the adult retroperitoneal position (1). The perirenal space is divided into multiple compartments by thin fibrous lamellae and bridging septa (Kunin septa) that connect the renal capsule with the anterior and posterior renal fasciae (3). The perirenal space abuts the bare area of the liver on the right and the subphrenic space on the left. The anterior renal fascia, which overlies the upper portion of the right kidney and adrenal gland, may be deficient and allow communication of the perirenal space with the hepatic bare area (4). The left and right perirenal spaces communicate with each other across the midline and with the pelvic retroperitoneal spaces below the iliac fossa. The perirenal space contains the kidneys, adrenal glands, proximal ureters, perirenal fat, lymphatic vessels, and blood vessels (1) (Fig 1).

The perirenal space is commonly involved in a wide variety of neoplastic and nonneoplastic conditions (Table 1). Perirenal tumors and pseudotumors may arise from the kidney or as part of a disease process that affects multiple organs. In this article, we describe the imaging features of a heterogeneous group of perirenal lesions and propose an imaging pattern–based approach to their characterization (Table 2).

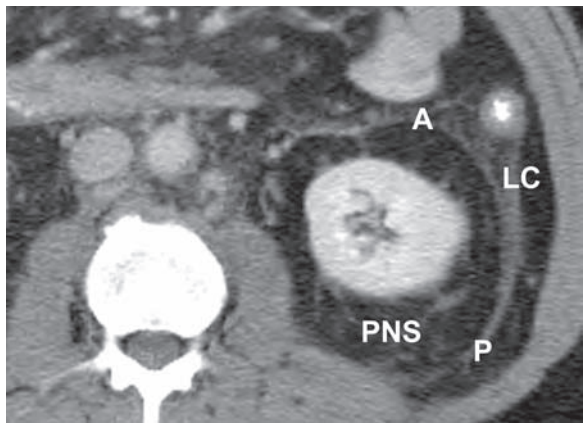

Figure 1. Axial contrast-enhanced CT scan in a patient with acute pancreatitis shows the cross-sectional anatomy of the left perinephric space *(PNS)*, with its anterior limit *(A)* marked by the Gerota fascia and its posterior limit *(P)* by the Zuckerkandl fascia. *LC* = lateroconal fascia.

Table 1
Spectrum of Proliferative Tumors and Pseudotumors of the Perirenal Space

Primary lesions
Lymphoma
Leukemia
Extramedullary hematopoiesis
Metastases (bronchogenic carcinoma)
Castleman disease
Extraadrenal myelolipoma
Erdheim-Chester disease
Renal lesions with extension
Renal cell carcinoma
Angiomyolipoma
Xanthogranulomatous pyelonephritis
Leiomyoma
Hemangioma
Lymphangioma
Retroperitoneal lesions with extension
Lymphoma
Leukemia
Metastatic lymphadenopathy
Malignant fibrous histiocytoma
Liposarcoma
Plasma cell neoplasms
Retroperitoneal fibrosis

Solitary Soft-Tissue Masses

Renal Adenocarcinoma

Renal adenocarcinomas are the most common malignant neoplasms of the kidneys. They have variable histologic features, biologic behavior, and imaging findings (5).

Renal adenocarcinoma with perinephric spread constitutes the most commonly occurring perirenal soft-tissue mass. The clear cell variant is the most frequently seen at histologic analysis (approximately 60%–80% of cases). Clear cell carcinoma typically is hypervascular but shows heterogeneous enhancement at computed tomography (CT) and magnetic resonance (MR) imaging (5) (Fig 2). Other subtypes, such as papillary (10%–15% of cases) and chromophobe (5%–10% of cases) carcinomas, are typically hypovascular and show relatively homogeneous contrast enhancement. Accurate preoperative staging of renal adenocarcinoma permits optimal patient management. In addition, local staging is helpful for determining the best surgical approach

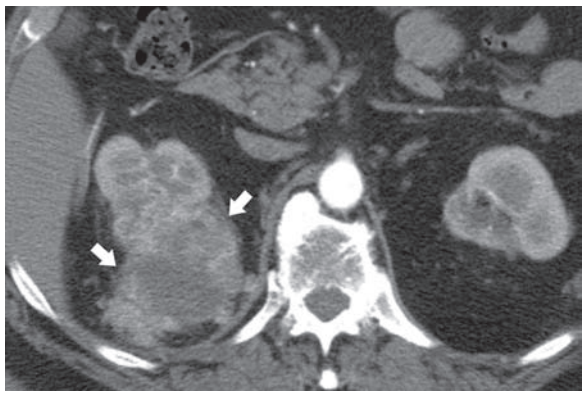

Figure 2. Renal cell carcinoma with perirenal extension. Axial contrast-enhanced CT scan shows a heterogeneously enhancing right renal mass (arrows) with extracapsular spread.

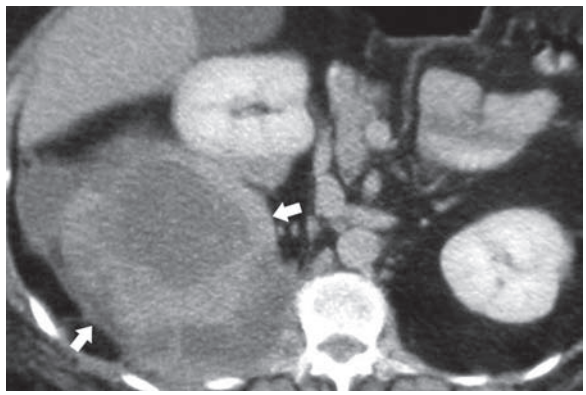

Figure 3. Perirenal malignant fibrous histiocytoma. Axial contrast-enhanced CT scan shows a heterogeneous solid mass (arrows) with internal areas of low attenuation.

Table 2
Imaging Pattern–based Characterization of Perirenal Tumors and Pseudotumors

Solitary perirenal mass
Renal cell carcinoma with perirenal spread
Malignant fibrous histiocytoma
Leukemia
Lymphoma
Castleman disease
Leiomyoma
Hemangioma
Lymphangioma
Rindlike soft-tissue perirenal mass
Lymphoma
Leukemia
Retroperitoneal fibrosis
Extramedullary hematopoiesis
Erdheim-Chester disease
Perirenal mass with macroscopic fat
Angiomyolipoma
Liposarcoma
Extramedullary hematopoiesis
Extraadrenal myelolipoma
Multiple perirenal masses
Metastases
Plasma cell neoplasms

and procedure (laparoscopic versus open incision). Whereas stage T2 tumors are resected by using an anterior approach, stage T3 tumors are resected with a retroperitoneal approach. Contrast-enhanced CT and MR imaging have high sensitivity, specificity, and accuracy for staging of renal adenocarcinomas and detection of their extracapsular spread (6,7). In a study of 15 patients with Robson stage I renal carcinoma, Catalano et al (7) found 96% sensitivity, 93% specificity, and 95% accuracy for the diagnosis of perirenal fat invasion based on the depiction of hyperattenuating streaks and soft-tissue nodules on CT scans. However, precise delineation of perinephric fat invasion and differentiation of the renal capsule from the tumor pseudocapsule may be difficult in some cases.

Malignant Fibrous Histiocytoma

Malignant fibrous histiocytoma is the most common soft-tissue sarcoma in adults. Approximately 15% of cases occur in the retroperitoneum (8). The lesions typically are characterized by areas of spindle cells arranged in a storiform pattern and by pleomorphic areas with haphazardly arranged sheets of fibroblasts and histiocytes. However, malignant fibrous histiocytoma is a heterogeneous disease with distinct histologic subtypes. In addition to the storiform-pleomorphic subtype (the most common), myxoid, giant cell, inflammatory, and angiomatoid variants have been described in the literature (9).

At imaging, retroperitoneal malignant fibrous histiocytoma appears as a large heterogeneous mass that contains areas of necrosis and hemorrhage (Fig 3). The mass frequently displaces the kidney and other retroperitoneal structures. Calcification is seen in 7%–20% of retroperitoneal malignant fibrous histiocytomas (8,10,11).

Renal Infections

Although renal infections are not proliferative disorders, some infectious conditions (eg, focal pyelonephritis and xanthogranulomatous infection) may be mistaken for neoplastic disorders of the kidney and the perinephric space. Acute pyelonephritis may result either from an ascending infection secondary to a urinary tract obstruction or from hematogenous dissemination.

Patient demographics and clinical and laboratory findings are frequently diagnostic of acute pyelonephritis. However, CT usually is performed to detect underlying predisposing factors, confirm the diagnosis of acute pyelonephritis in atypical cases, and assess complications such as abscess formation (12,13) (Fig 4).

Xanthogranulomatous pyelonephritis is a rare form of unilateral chronic pyelonephritis that is characterized by progressive parenchymal destruction and subsequent diffuse replacement by a macrophage-rich inflammatory infiltrate. The condition typically affects perimenopausal women with a history of recurrent urinary tract infections, diabetes mellitus, or obstructing calculi (14). Its diagnosis is challenging because clinical symptoms and laboratory findings are nonspecific. Typical CT findings include enlargement of the kidney, heterogeneous parenchymal enhancement or nonenhancement, hydronephrosis, abscesses, and obstructive staghorn-like calculi (14) (Fig 5). Extension of the inflammatory process into the perinephric space and retroperitoneum may simulate an infiltrative malignancy. In addition, the diagnosis of focal disease in the absence of obstructive calculi is difficult and may be made only at histopathologic examination. Diffuse xanthogranulomatous pyelonephritis is treated with an extended open nephrectomy, but focal disease is managed with a partial nephrectomy (14,15).

Hemangiopericytoma

Hemangiopericytoma is an uncommon retroperitoneal soft-tissue neoplasm that is hypothesized to arise from Zimmerman pericytes (16). The lesions most commonly occur in the extremities, particularly the thigh; the retroperitoneum is the second most common site. Hemangiopericytomas exhibit widely varying degrees of histologic and biologic aggressiveness (16,17).

Most retroperitoneal hemangiopericytomas appear as large, lobulated, well-circumscribed, hypervascular soft-tissue masses with foci of calcification and areas of necrosis (17). Displacement of the abdominopelvic viscera is more common than frank tissue invasion. Perinephric extension of retroperitoneal hemangiopericytomas frequently causes displacement of the kidneys. Preoperative embolization may be useful in some cases to reduce postoperative morbidity and achieve better resection; however, local and distant recurrences and metastases may occur. Ten-year survival rates of 47%–86% have been reported (17,18).

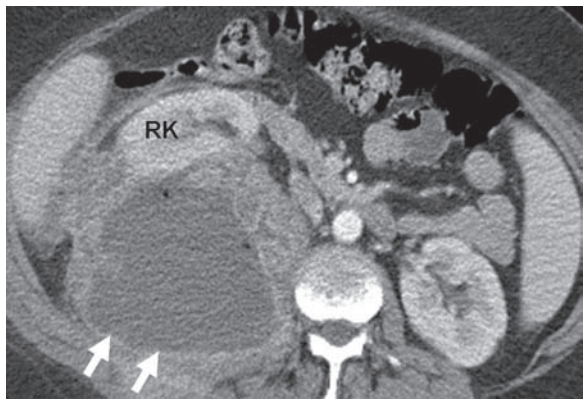

Figure 4. Perirenal abscess. Axial contrast-enhanced CT scan demonstrates a large abscess (arrows) that displaces the right kidney *(RK)* in the anterior direction.

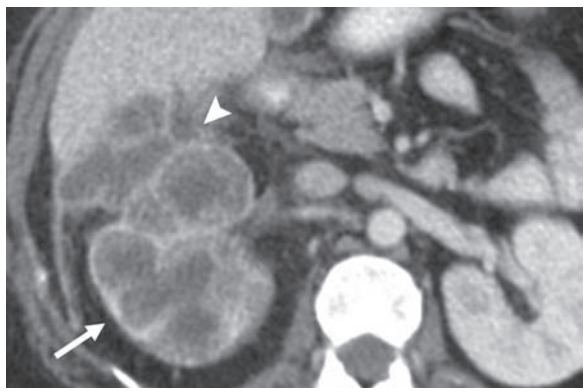

Figure 5. Focal xanthogranulomatous pyelonephritis. Axial contrast-enhanced CT scan shows nonenhancement of the right kidney (arrow) with anterior extension of the infectious process (arrowhead).

Leukemia

Leukemic involvement of the kidney is rare and may manifest at imaging as a diffusely infiltrating renal mass, a focal renal mass, or a perirenal mass (19,20). Granulocytic sarcomas (chloromas) are uncommon malignant neoplasms of granulocytic precursors that occur in up to 10% of patients with acute myelogenous leukemia. They are less commonly associated with acute lymphocytic leukemia. Renal chloromas appear as focal hypovascular soft-tissue masses in one or both kidneys (20). Perirenal leukemia occurs either as a result of perinephric extension of a renal lesion or, less commonly, as isolated leukemic involvement (Fig 6). The imaging findings are nonspecific, and a biopsy is required to obtain a definitive diagnosis (20).

Castleman Disease

Castleman disease is an uncommon idiopathic lymphoproliferative condition. Approximately 10%–15% of cases of Castleman disease occur in the abdomen and the retroperitoneum (21).

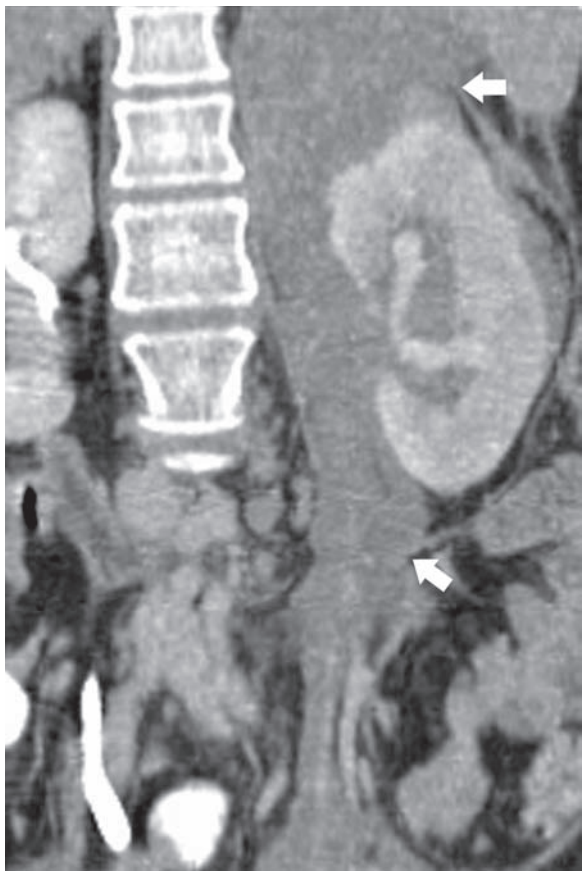

Figure 6. Perirenal and periureteral spread of leukemia. Coronal contrast-enhanced CT scan demonstrates a soft-tissue mass (arrows) that encases the left kidney and ureter.

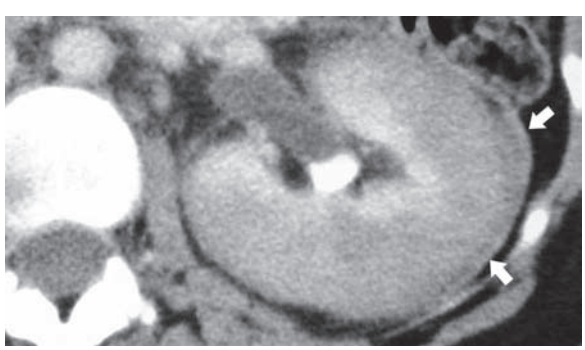

Figure 7. Castleman disease. Axial contrast enhanced CT scan depicts a diffuse hypoattenuating mass that involves the left kidney and extends into the perinephric space (arrows).

Isolated perirenal lesions are uncommon. Castleman disease is classified as either hyaline-vascular subtype or plasma cell subtype on the basis of histologic findings and as either unicentric or multicentric on the basis of clinical manifestations (21). Multicentric Castleman disease is associated with Kaposi sarcoma from herpesvirus infection and is commonly seen in patients with

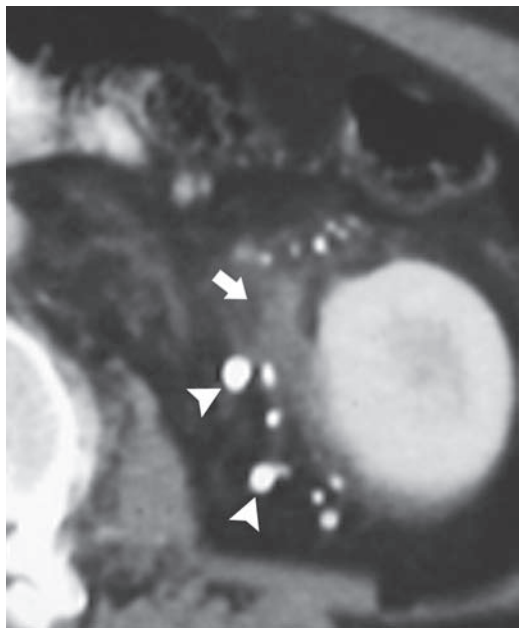

Figure 8. Perirenal hemangioma. Axial contrast-enhanced CT scan shows a left perirenal soft-tissue mass (arrow) with associated phleboliths (arrowheads).

acquired immunodeficiency syndrome. Multicentric Castleman disease is biologically more aggressive and is associated with a poor prognosis.

Imaging findings vary with the clinical and histologic subtype. Unicentric Castleman disease manifests as a well-defined, homogeneous, solitary intraabdominal mass with soft-tissue attenuation (22,23). Multicentric Castleman disease manifests in diffuse lymphadenopathy, hepatosplenomegaly, and ascites (21). Renal and perirenal involvement in the disease is rare (Fig 7). Findings of calcification, intense contrast enhancement, and central fibrosis favor a classification of hyaline-vascular subtype over that of plasma cell subtype (21,24).

Perirenal Hemangioma

Hemangiomas of the kidney are rare benign mesenchymal renal neoplasms that occur most often in the medulla and the renal sinus region (25). Most renal hemangiomas are solitary, small, and unilateral. Retroperitoneal and perirenal hemangiomas are extremely rare (26).

Imaging features of renal or perirenal hemangiomas are variable. The depiction of a soft-tissue mass with phleboliths, high signal intensity on T2-weighted MR images, and delayed or persistent contrast enhancement is suggestive of the diagnosis (25,27) (Fig 8). However, the imaging characteristics of renal and perirenal

Teaching Point

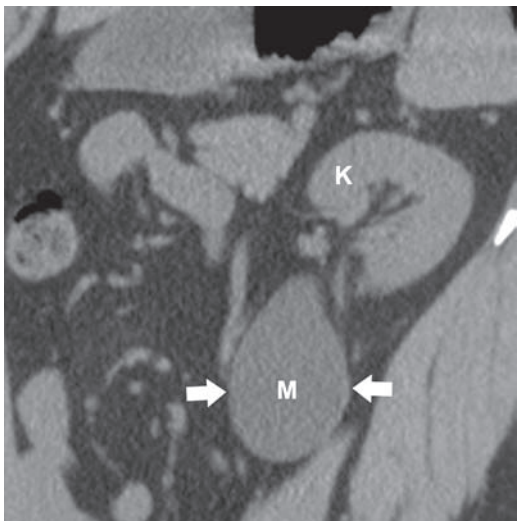

Figure 9. Perirenal lymphangioma. Sagittal unenhanced CT scan shows a well-circumscribed cystic perirenal mass *(M)* (arrows). *K* = kidney.

hemangiomas are nonspecific and may mimic those of transitional cell carcinoma or renal cell carcinoma (25,26).

Perirenal Lymphangioma

Renal and perirenal lymphangiomas are rare benign mesenchymal neoplasms that are histologically characterized by intercommunicating endothelium-lined spaces (28). The lesions may be unilateral or bilateral and diffuse or focal. At imaging, perirenal lymphangioma has the appearance of a uni- or multilocular cystic lesion with or without associated peripheral or septal enhancement (29,30) (Fig 9). Perirenal lymphangiomatosis is characterized by involvement of the entire perirenal mesenchyme, with bilateral perinephric cystic masses (31).

Renal Leiomyoma

Renal leiomyomas are rare benign mesenchymal neoplasms that mostly occur in asymptomatic adults. Perirenal leiomyomas are essentially exophytic renal tumors that arise from the renal capsule and extend into the perirenal space (32) (Fig 10). Imaging findings include a well-circumscribed soft-tissue mass that is supplied by renal capsular vessels (32). Larger leiomyomas are heterogeneous in appearance because of hemorrhage and cystic-myxoid degeneration (33).

Extragastrointestinal Stromal Tumor

The gastrointestinal stromal tumor (GIST) is a nonepithelial neoplasm that may originate from

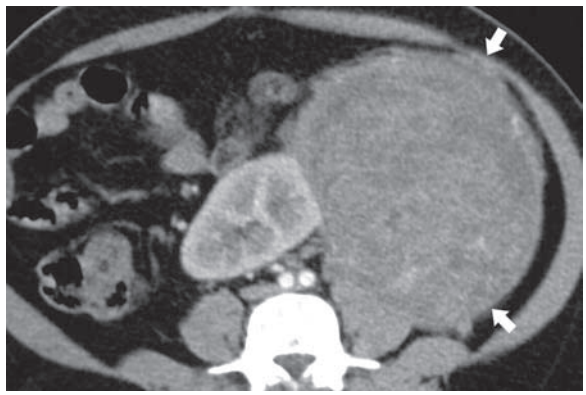

Figure 10. Renal leiomyoma. Axial contrast-enhanced CT scan depicts an exophytic soft-tissue mass (arrows) arising from the capsule of the left kidney.

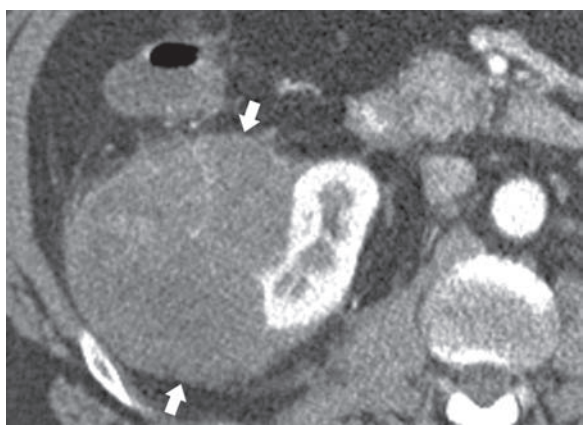

Figure 11. Primary extragastrointestinal stromal tumor in the perinephric space. Axial contrast-enhanced CT scan demonstrates a soft-tissue mass (arrows) that has invaded the right kidney.

the c-KIT–positive interstitial cells of Cajal, the pacemaker cells of the gastrointestinal tract, where most GISTs are located. GISTs that occur outside the gastrointestinal tract are known as extragastrointestinal stromal tumors (34,35). Primary extragastrointestinal stromal tumors are extremely rare in perirenal locations; most are found in the omentum and mesentery (35). Perirenal extragastrointestinal stromal tumors appear as hypovascular soft-tissue masses (Fig 11). Their imaging features are nonspecific, and a biopsy is required for accurate diagnosis.

Rindlike Soft-Tissue Masses

Lymphoma

Perirenal involvement in lymphoma is usually due to contiguous spread from retroperitoneal or renal lymphoma. The occurrence of isolated lymphoma in the perirenal space is very unusual (<10% of cases of perirenal lymphoma) (36).

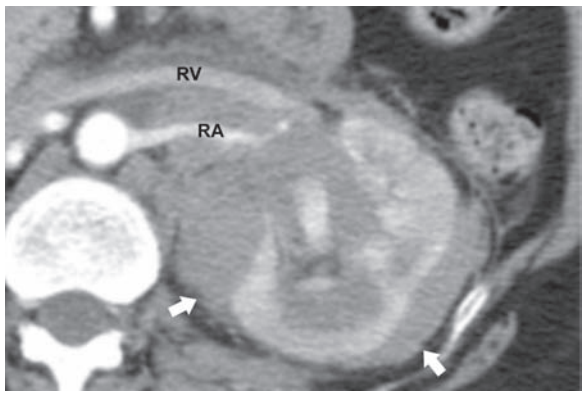

Figure 12. Perirenal lymphoma. Axial contrast enhanced CT scan demonstrates a soft-tissue mass (arrows) that has encased the left kidney and renal vessels. *RA* = renal artery, *RV* = renal vein.

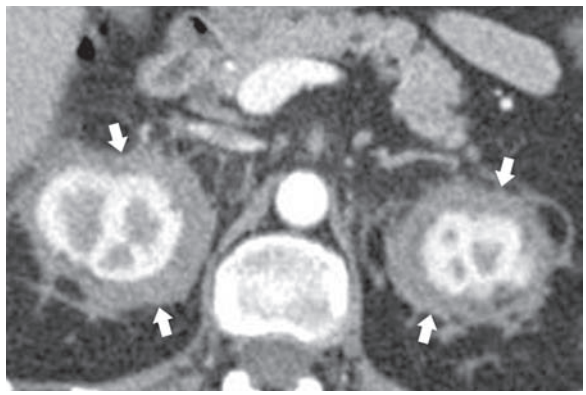

Figure 13. Perirenal fibrosis in a patient with scleroderma. Axial contrast-enhanced CT scan obtained during the corticomedullary phase depicts a rindlike soft-tissue layer surrounding both kidneys (arrows).

Renal involvement in lymphoma occurs much more commonly in non-Hodgkin disease, with the majority of patients having intermediate or high-grade lymphomas of B-cell origin (37). However, in most cases of Hodgkin lymphoma with perirenal involvement, the renal parenchyma is not involved (38).

Renal lymphomas show several distinct imaging patterns: multiple masses, a solitary mass, a diffuse infiltrating renal mass, a rindlike soft-tissue thickening around the kidneys, and direct invasion from adjacent retroperitoneal lymphadenopathy (37). Isolated perirenal lymphoma appears as a uniformly attenuating rindlike soft-tissue mass around the kidney (Fig 12). The mass may invade or compress the kidney without significantly affecting renal function (37).

Retroperitoneal Fibrosis

Retroperitoneal fibrosis is characterized by a proliferation of fibrous tissue around the aorta. The fibrous layer extends along the aorta through a plaquelike infiltrative soft-tissue process (39). Retroperitoneal fibrosis typically is localized to the distal abdominal (infrarenal) aorta and the common iliac arteries; involvement of the pelvis is uncommon (39). About two-thirds of cases are idiopathic (39). There is a 3:1 male-to-female preponderance among those affected by the disease (40).

Retroperitoneal fibrosis may be considered as an isolated disease or as part of a systemic syndrome known as multifocal fibrosclerosis, which also may include autoimmune pancreatitis, sclerosing cholangitis, scleroderma, Riedel thyroiditis, fibrotic pseudotumor of the orbit, and fibrosis involving multiple organ systems (40). Perirenal involvement may be secondary to extension from retroperitoneal fibrosis (41), may occur without associated retroperitoneal fibrosis (39,42), or may be one of various manifestations of multifocal fibrosclerosis (40,43).

Three stages of the disease have been described, ranging from chronic active inflammation to fibrous scarring (39). Typical imaging manifestations of perirenal fibrosis include a soft-tissue mass that envelops the kidneys without displacing them (40) (Fig 13). The T2-weighted MR signal intensity and dynamic enhancement characteristics depend on the stage of the disease. Whereas areas affected by active inflammation demonstrate high T2 signal intensity and early contrast enhancement, areas of fibrosis show low T2 signal intensity and delayed contrast enhancement (39). Perirenal fibrosis that occurs in association with retroperitoneal fibrosis or as part of multifocal fibrosclerosis is not difficult to detect at imaging. However, the imaging features of isolated perirenal fibrosis are nonspecific, and a biopsy may be required to achieve a definitive diagnosis (42).

Erdheim-Chester Disease

Erdheim-Chester disease is a rare form of systemic non–Langerhans cell histiocytosis of unknown etiology but with characteristic histologic and imaging findings (44). Histologically, Erdheim-Chester disease is defined by a mononuclear infiltrate consisting of lipid-laden, foamy histiocytes that stain positive for CD68 and negative for CD1a and S100 (45). Erdheim-Chester disease affects middle-aged individuals, without any specific sex predilection (46). Patients with the disease typically present with lower-extremity bone pain. Skeletal radiographic findings include bilateral symmetric metadiaphyseal cortical thickening,

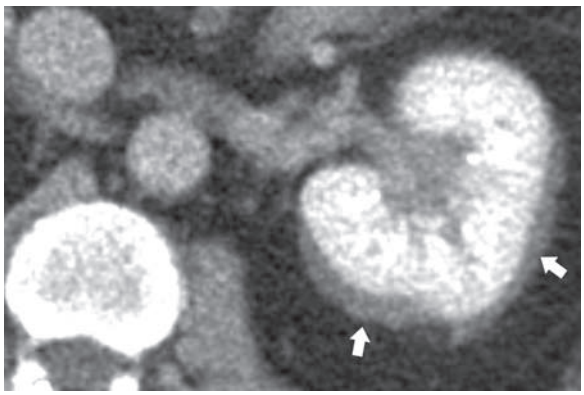

Figure 14. Erdheim-Chester disease. Axial contrast-enhanced CT scan obtained during the nephrographic phase shows a rindlike soft-tissue layer surrounding the left kidney (arrows).

a coarsened trabecular pattern, and medullary sclerosis in the long bones of the appendicular skeleton, with sparing of the epiphyses and axial skeleton (47). Extraskeletal manifestations, which include central nervous system involvement, are seen in about half of those affected (46). Other organs in which involvement has been reported include the lungs, skin, kidneys, retroperitoneum, and heart (48).

Teaching Point

Perirenal involvement in Erdheim-Chester disease characteristically is manifested as rindlike soft-tissue lesions surrounding the kidneys and ureters (45,49,50) (Fig 14). Severe compression of the renal parenchyma and ureters because of fibrous perinephritis leads to progressive renal failure (50). Percutaneous nephrostomy is difficult because of fibrous perinephritis. Ureteral stent placement and systemic corticosteroid therapy are the standard treatments until active inflammation resolves (49).

Multiple Soft-Tissue Masses

Perirenal Metastases

Metastases to the adrenal glands and kidneys are not uncommon. However, isolated perirenal metastases are rare. The perirenal space is an unusual but potentially significant site of metastases from lung cancer and other primary tumors such as malignant melanoma, breast carcinoma, and prostate cancer (51,52). Lung cancer shows a specific predilection for perirenal spread secondary to connections between the perirenal and mediastinal lymphatic vessels (1,51). At imaging, perirenal metastases frequently present as multiple soft-tissue masses around the kidney (52,53) (Fig 15).

Teaching Point

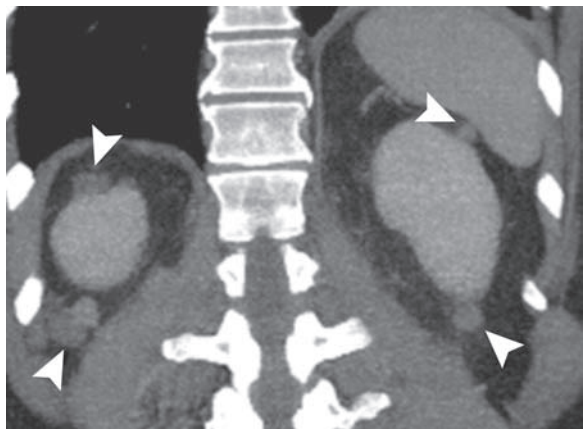

Figure 15. Perirenal metastases from bronchogenic carcinoma with mediastinal lymphadenopathy. Coronal contrast-enhanced CT scan shows multiple bilateral soft-tissue masses (arrowheads).

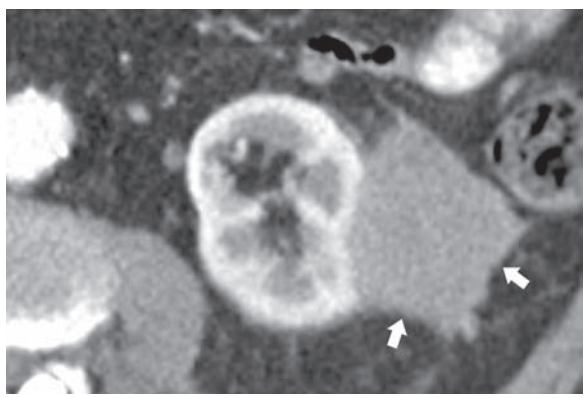

Figure 16. Perirenal plasmacytoma. Axial contrast-enhanced CT scan demonstrates a well-defined soft-tissue mass (arrows) that indents the left kidney.

Plasma Cell Neoplasms

Plasma cell neoplasms refers to a spectrum of malignant neoplasms that comprise multiple myeloma, plasmacytoma, and plasma cell leukemia (54). Although multiple myeloma originates in the bone marrow, it spreads to extramedullary sites in approximately 70% of patients (55,56). Plasmacytoma differs from multiple myeloma in that primary lesions may arise outside the bone marrow. Perirenal involvement in multiple myeloma manifests as multiple enhancing masses, whereas plasmacytoma manifests as a solitary enhancing mass with ill-defined margins (54,57,58) (Fig 16).

Macroscopic Fat–containing Masses

Angiomyolipoma

Angiomyolipoma is a benign unencapsulated mesenchymal neoplasm that is composed of

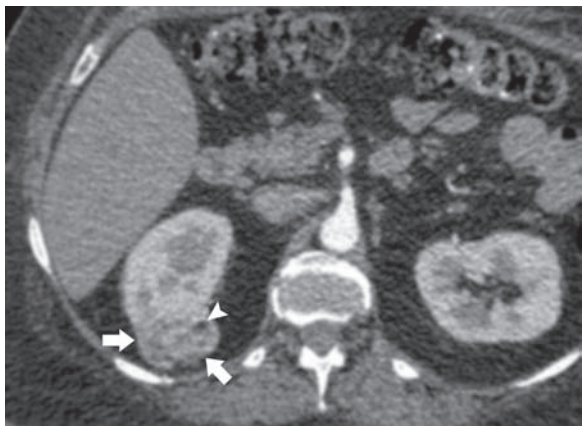

Figure 17. Renal angiomyolipoma. Axial contrast-enhanced CT scan shows an exophytic hypervascular right renal mass (arrows) with macroscopic fat (arrowhead).

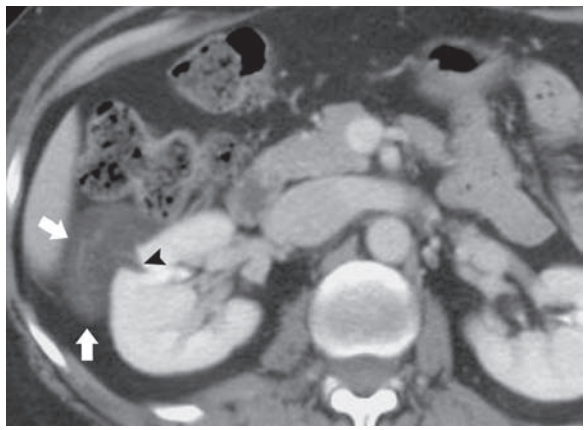

Figure 18. Renal angiomyolipoma. Axial contrast-enhanced CT scan demonstrates an exophytic fat-containing mass (arrows) that has arisen from the right kidney. Note the characteristic parenchymal defect (arrowhead).

smooth muscle cells, blood vessels, and adipose tissue in varying proportions (59). On the basis of a unifying histogenetic theory, angiomyolipomas are now considered within the category of neoplasms consisting of perivascular epithelioid cells (so-called PEComas) (60). Perirenal involvement usually results from perinephric extension of an angiomyolipoma of the kidney; primary perirenal angiomyolipoma arising from the perinephric mesenchyme is extremely rare (61). Primary perirenal angiomyolipomas have a strong female predilection and, like sporadic renal angiomyolipomas, are associated with an increased risk of hemorrhage.

Renal angiomyolipomas may occur either sporadically or as part of an autosomal dominant genetic disorder known as tuberous sclerosis complex. Sporadic renal angiomyolipomas are most often large, solitary, symptomatic tumors. Bilateral multiple renal angiomyolipomas occur in young patients (mean age, 25–35 years) with tuberous sclerosis complex. Because life-threatening hemorrhage and renal failure are common in those affected, angiomyolipomas are a significant cause of morbidity and mortality in adult patients with tuberous sclerosis complex (62). A subset of renal angiomyolipomas referred to as monotypic epithelioid angiomyolipomas may show aggressive biologic behavior including malignant transformation with regional or disseminated metastases, vascular invasion, local recurrence, and death (62). Epithelioid angiomyolipomas typically do not contain macroscopic fat and may not be distinguishable from renal cell carcinoma at imaging. A definitive diagnosis is based on a detailed histopathologic evaluation after resection or biopsy of the mass.

The imaging features of angiomyolipoma depend on the tumor size as well as the relative proportions of soft tissue, mature adipose tissue, and hypertrophied blood vessels within the tumor. Small angiomyolipomas appear homogeneous at cross-sectional imaging. Large angiomyolipomas are heterogeneous masses containing variable amounts of macroscopic fat, hypervascular soft tissue, and aneurysms (61,63) (Fig 17). The characteristic finding of macroscopic fat content is readily identified on CT scans or on frequency-selective fat-suppressed MR images (Fig 17). Renal angiomyolipoma with perinephric extension is the most common macroscopic fat–containing mass in the perirenal region. However, renal angiomyolipomas with minimal fat are indistinguishable from other renal soft-tissue masses, most notably renal cell carcinoma (64). Like renal angiomyolipoma, primary retroperitoneal angiomyolipoma demonstrates an increased propensity to bleed; the risk of hemorrhage correlates with the size of the tumor (59). Renal angiomyolipoma with perinephric extension must be distinguished from a primary retroperitoneal (perirenal) liposarcoma. The presence of a well-defined renal parenchymal defect and intralesional aneurysms are suggestive of a diagnosis of angiomyolipoma of the kidney rather than a liposarcoma (63) (Fig 18).

Teaching Point

Teaching Point

Liposarcoma

Liposarcoma is the most common primary retroperitoneal malignant neoplasm. There are five histologic subtypes: well differentiated, myxoid, round cell, pleomorphic, and dedifferentiated (65). Retroperitoneal liposarcomas are typically well differentiated or dedifferentiated (with

frequent genetic amplification of the 12q13-15 region) and are commonly large at presentation (66). Dedifferentiation also is commonly seen (10%–15% of cases) because of the long latent period before diagnosis (66). There is no specific sex predilection, and the peak occurrence is in the 6th and 7th decades of life (between 51 and 70 years of age).

Imaging findings commonly reflect histologic features. Well-differentiated liposarcomas have a predominant macroscopic fat component, whereas round cell and pleomorphic types appear as soft-tissue masses (Fig 19) (65,67). Myxoid liposarcoma appears cystic, with reticular enhancement after contrast material is administered. The surgical resection of retroperitoneal liposarcomas is technically difficult because of their large size, and a high rate of local recurrence (90%) has been reported (66). Well-differentiated liposarcomas are biologically less aggressive; the myxoid subtype has an intermediate prognosis; and the round cell and pleomorphic subtypes are considered high grade, with high rates of local recurrence and metastasis (66,67).

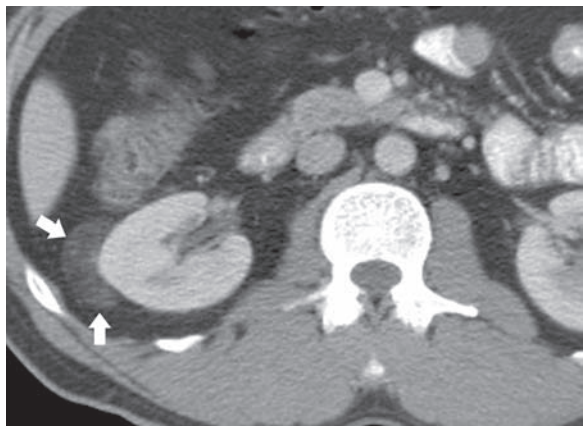

Figure 19. Perirenal liposarcoma. Axial contrast-enhanced CT scan shows a well-circumscribed mass with predominant fat content (arrows). The mass is localized in the right perirenal space.

Extramedullary Hematopoiesis

Extramedullary hematopoiesis occurs when hematopoietic tissue develops outside primary (medullary) sites. Such occurrences may be associated with hemolytic anemia, hemoglobinopathies, primary and secondary myelofibrosis, leukemia, lymphoma, or skeletal metastases (68). The most common sites of extramedullary hematopoiesis are the liver, spleen, and paraspinal regions of the thorax, a distribution that reflects the various levels of hematopoietic activity in these sites during embryogenesis (69). Extramedullary hematopoiesis also has been reported in various other sites, including lymph nodes, mediastinum, central nervous system, pleura and lungs, heart, gastrointestinal tract, and kidneys (69,70).

Perirenal involvement in extramedullary hematopoiesis is uncommon and manifests one of two distinct imaging patterns: a diffuse infiltrative process surrounding the kidneys, or soft-tissue masses intermixed with macroscopic fat (68,70,71). On CT scans, extramedullary hematopoiesis appears as a hypovascular soft-tissue mass with or without associated macroscopic fat (Fig 20). On T2-weighted MR images, the soft-tissue component has a characteristic low signal intensity because of its hemosiderin content (71).

Perirenal extramedullary hematopoiesis poses particular diagnostic difficulty when it occurs in unusual sites because the imaging findings may resemble those of other neoplasms. The diffuse infiltrative type typically mimics lymphoma, whereas the macroscopic fat–containing type resembles other fatty neoplasms (71). The diagnosis therefore is usually established at histopathologic analysis.

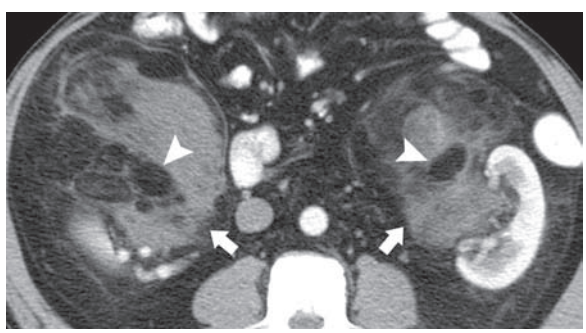

Figure 20. Extramedullary hematopoiesis. Axial contrast-enhanced CT scan shows large bilateral perirenal heterogeneous masses (arrows) with predominant fatty components (arrowheads).

Extraadrenal Myelolipoma

Myelolipomas are rare benign monoclonal neoplasms composed of an admixture of mature adipose tissue and normal hematopoietic cells (72). Four distinct types of myelolipomas have been described: isolated adrenal myelolipoma, adrenal myelolipoma with hemorrhage, extraadrenal myelolipoma, and myelolipoma associated with other adrenal disease (73). The adrenal gland is the most common target site of myelolipoma. Extraadrenal myelolipomas are distinctly rare but their occurrence has been described in the retroperitoneum, stomach, liver, lung, presacral area,

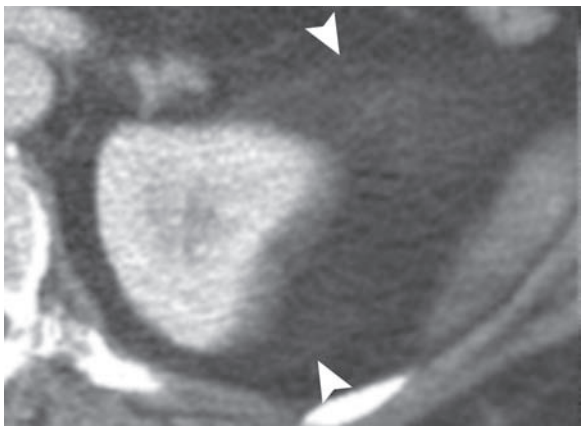

Figure 21. Perirenal myelolipoma. Axial contrast-enhanced CT scan demonstrates an indistinct fatty mass (arrowheads) that indents the left kidney and merges with the adjacent retroperitoneal fat.

and mediastinum. Extraadrenal myelolipoma shows a particular predilection for involving the perirenal and presacral regions (74). On average, patients with extraadrenal myelolipoma are a decade older (mean age, 64 years) than those with adrenal myelolipoma (mean age, 55 years). Extraadrenal lesions seem slightly more common in females (75).

Imaging findings depend on the proportions of the adipose and hematopoietic tissue contents. Myelolipomas typically appear heterogeneous, with both hypervascular soft-tissue and macroscopic fat components depicted on CT scans and MR images (75,76). The presence of macroscopic fat is a characteristic finding in myelolipoma (Fig 21) (75). Whereas adrenal myelolipomas are readily diagnosed on the basis of their imaging appearance and location, extraadrenal myelolipomas may be mistaken for other fat-containing masses. The diagnosis is usually established at histopathologic analysis.

Summary

A wide spectrum of neoplastic and nonneoplastic proliferative conditions may involve the perirenal space either in isolation or as part of a systemic disease process. Perirenal localization may be the predominant or the only site of involvement in a systemic condition. Although some tumors and pseudotumors of the perirenal space (eg, angiomyolipoma, hemangioma, and lymphangioma) have characteristic imaging findings that permit their diagnosis, a biopsy and histopathologic evaluation are required in most cases to establish a definitive diagnosis. Nevertheless, familiarity with the spectrum of imaging features of perirenal tumors and pseudotumors may facilitate accurate diagnosis and timely treatment.

References

1. Gore RM, Balfe DM, Aizenstein RI, Silverman PM. The great escape: interfascial decompression planes of the retroperitoneum. AJR Am J Roentgenol 2000;175:363–370.
2. Thornton FJ, Kandiah SS, Monkhouse WS, Lee MJ. Helical CT evaluation of the perirenal space and its boundaries: a cadaveric study. Radiology 2001;218:659–663.
3. Kunin M. Bridging septa of the perinephric space: anatomic, pathologic, and diagnostic considerations. Radiology 1986;158:361–365.
4. Kim KW, Auh YH, Chi HS, Lee SI. CT of retroperitoneal extension of hepatoma mimicking adrenal tumor. J Comput Assist Tomogr 1993;17:599–602.
5. Prasad SR, Humphrey PA, Catena JR, et al. Common and uncommon histologic subtypes of renal cell carcinoma: imaging spectrum with pathologic correlation. RadioGraphics 2006;26:1795–1806; discussion 1806–1810.
6. Kamel IR, Hochman MG, Keogan MT, et al. Accuracy of breath-hold magnetic resonance imaging in preoperative staging of organ-confined renal cell carcinoma. J Comput Assist Tomogr 2004;28:327–332.
7. Catalano C, Fraioli F, Laghi A, et al. High-resolution multidetector CT in the preoperative evaluation of patients with renal cell carcinoma. AJR Am J Roentgenol 2003;180:1271–1277.
8. Neville A, Herts BR. CT characteristics of primary retroperitoneal neoplasms. Crit Rev Comput Tomogr 2004;45:247–270.
9. Fletcher CD, Gustafson P, Rydholm A, Willen H, Akerman M. Clinicopathologic re-evaluation of 100 malignant fibrous histiocytomas: prognostic relevance of subclassification. J Clin Oncol 2001;19:3045–3050.
10. Sawada Y, Yamamoto S, Ogawa T, Ohkawa T. Malignant fibrous histiocytoma of the perirenal tissue: report of a case—a statistical study of 58 cases of urological malignant fibrous histiocytoma in Japanese literature [in Japanese]. Hinyokika Kiyo 1986;32:853–864.
11. Tomita M, Shimomura T, Ito H, Ikemoto I, Oishi Y. Malignant fibrous histiocytoma of perirenal tissue: a case report [in Japanese]. Hinyokika Kiyo 2002;48:327–329.
12. Demertzis J, Menias CO. State of the art: imaging of renal infections. Emerg Radiol 2007;14:13–22.
13. Stunell H, Buckley O, Feeney J, Geoghegan T, Browne RF, Torreggiani WC. Imaging of acute pyelonephritis in the adult. Eur Radiol 2007;17:1820–1828.
14. Loffroy R, Guiu B, Watfa J, Michel F, Cercueil JP, Krause D. Xanthogranulomatous pyelonephritis in adults: clinical and radiological findings in diffuse and focal forms. Clin Radiol 2007;62:884–890.
15. Osca JM, Peiro MJ, Rodrigo M, Martinez-Jabaloyas JM, Jimenez-Cruz JF. Focal xanthogranulomatous pyelonephritis: partial nephrectomy as definitive treatment. Eur Urol 1997;32:375–379.
16. Enzinger FM, Smith BH. Hemangiopericytoma: an analysis of 106 cases. Hum Pathol 1976;7:61–82.

17. Goldman SM, Davidson AJ, Neal J. Retroperitoneal and pelvic hemangiopericytomas: clinical, radiologic, and pathologic correlation. Radiology 1988;168:13–17.
18. Arnoletti P, Jhala N. Retroperitoneal hemangiopericytoma. J Am Coll Surg 2003;197:687–688.
19. Araki T. Leukemic involvement of the kidney in children: CT features. J Comput Assist Tomogr 1982;6:781–784.
20. Marcos HB, Semelka RC, Woosley JT. Abdominal granulocytic sarcomas: demonstration by MRI. Magn Reson Imaging 1997;15:873–876.
21. Enomoto K, Nakamichi I, Hamada K, et al. Unicentric and multicentric Castleman's disease. Br J Radiol 2007;80:e24–e26.
22. Okada S, Maeta H, Maeba T, Goda F, Mori S. Castleman disease of the pararenal retroperitoneum: report of a case. Surg Today 1999;29:178–181.
23. Takihara H, Yamakawa G, Baba Y, Takahashi M, Ishihara T. Castleman disease: unusual retroperitoneal location indistinguishable from malignant tumor in preoperative angiographic appearance. Urology 1993;41:162–164.
24. Germaine LM, Newhouse JH. Castleman's disease. Clin Imaging 2003;27:431–434.
25. Prasad SR, Humphrey PA, Menias CO, et al. Neoplasms of the renal medulla: radiologic-pathologic correlation. RadioGraphics 2005;25:369–380.
26. Okuno T, Ando M, Arisawa C, Okano T. A case of perirenal hemangioma mimicking renal cell carcinoma. Int J Urol 1999;6:104–106.
27. Higuchi R, Yamaguchi Y, Shoji T, Wakasugi S, Takahashi H, Fujita R. A mediastinal hemangioma, associated with perirenal hemangioma and congenital anomaly of the inferior vena cava. Intern Med 2000;39:1083–1087.
28. Eble JN, Sauter G, Epstein JI, Sesterhenn IA, eds. World Health Organization classification of tumours: pathology and genetics of tumours of the urinary system and male genital organs. Lyon, France: IARC, 2004.
29. Mani NB, Sodhi KS, Singh P, Katariya S, Poddar U, Thapa BR. Renal lymphangiomatosis: a rare cause of bilateral nephromegaly. Australas Radiol 2003;47:184–187.
30. Zapzalka DM, Krishnamurti L, Manivel JC, DiSandro MJ. Lymphangioma of the renal capsule. J Urol 2002;168:220.
31. Varela JR, Bargiela A, Requejo I, Fernandez R, Darriba M, Pombo F. Bilateral renal lymphangiomatosis: US and CT findings. Eur Radiol 1998;8:230–231.
32. Lee SY, Hsu HH, Chang CT, Yang CW, Wong YC, Wang LJ. Renal capsular leiomyoma—imaging features on computed tomography and angiography. Nephrol Dial Transplant 2006;21:228–229.
33. Nagar AM, Raut AA, Narlawar RS, Bhatgadde VL, Rege S, Thapar V. Giant renal capsular leiomyoma: study of two cases. Br J Radiol 2004;77:957–958.
34. Takao H, Yamahira K, Doi I, Watanabe T. Gastrointestinal stromal tumor of the retroperitoneum: CT and MR findings. Eur Radiol 2004;14:1926–1929.
35. Miettinen M, Monihan JM, Sarlomo-Rikala M, et al. Gastrointestinal stromal tumors/smooth muscle tumors (GISTs) primary in the omentum and mesentery: clinicopathologic and immunohistochemical study of 26 cases. Am J Surg Pathol 1999;23:1109–1118.
36. Reznek RH, Mootoosamy I, Webb JA, Richards MA. CT in renal and perirenal lymphoma: a further look. Clin Radiol 1990;42:233–238.
37. Sheth S, Ali S, Fishman E. Imaging of renal lymphoma: patterns of disease with pathologic correlation. RadioGraphics 2006;26:1151–1168.
38. Guermazi A, Brice P, de Kerviler EE, et al. Extranodal Hodgkin disease: spectrum of disease. RadioGraphics 2001;21:161–179.
39. Triantopoulou C, Rizos S, Bourli A, Koulentianos E, Dervenis C. Localized unilateral perirenal fibrosis: CT and MRI appearances. Eur Radiol 2002;12:2743–2746.
40. Szarf G, Bluemke DA. Case 83: multifocal fibrosclerosis with mediastinal-retroperitoneal involvement. Radiology 2005;235:829–832.
41. Barrett RL, Horrow MM, Gubernick JA, Rosenberg HK. US case of the day. Retroperitoneal fibrosis with perirenal involvement. RadioGraphics 1995;15:1024–1026.
42. Ergen FB, Arslan EB, Turkbey B, Akinci D, Akata D. Unilateral perirenal fibrosis. J Comput Assist Tomogr 2005;29:477–480.
43. Emch TM, Miller MA. Retroperitoneal fibrosis involving the left kidney in a patient with a remote history of Riedel's thyroiditis. AJR Am J Roentgenol 2005;184(3 suppl):S97–S98.
44. Gomez C, Diard F, Chateil JF, Moinard M, Dousset V, Rivel J. Imaging of Erdheim-Chester disease [in French]. J Radiol 1996;77:1213–1221.
45. Yun EJ, Yeh BM, Yabes AP, Coakley FV, Kane CJ. Erdheim-Chester disease: case report and review of associated urological, radiological and histological features. J Urol 2003;169:1470–1471.
46. Sheu SY, Wenzel RR, Kersting C, Merten R, Otterbach F, Schmid KW. Erdheim-Chester disease: case report with multisystemic manifestations including testes, thyroid, and lymph nodes, and a review of literature. J Clin Pathol 2004;57:1225–1228.

47. Bancroft LW, Berquist TH. Erdheim-Chester disease: radiographic findings in five patients. Skeletal Radiol 1998;27:127–132.
48. Fortman BJ, Beall DP. Erdheim-Chester disease of the retroperitoneum: a rare cause of ureteral obstruction. AJR Am J Roentgenol 2001;176: 1330–1331.
49. Murray D, Marshall M, England E, Mander J, Chakera TM. Erdheim-Chester disease. Clin Radiol 2001;56:481–484.
50. Wimpissinger TF, Schernthaner G, Feichtinger H, Stackl W. Compression of kidneys in Erdheim-Chester disease of retroperitoneum: open surgical approach. Urology 2005;65:798.
51. Wilbur AC, Turk JN, Capek V. Perirenal metastases from lung cancer: CT diagnosis. J Comput Assist Tomogr 1992;16:589–591.
52. Grutzner G, Jungblut RM. Perirenal metastasis of a malignant melanoma in a young child [in German]. Aktuelle Radiol 1993;3:372–374.
53. Koutani A, Lechevallier E, Andre M, de Fromont M, Coulange C. Contralateral perirenal metastasis of renal adenocarcinoma [in French]. Prog Urol 1997;7:1002–1003.
54. Monill J, Pernas J, Montserrat E, et al. CT features of abdominal plasma cell neoplasms. Eur Radiol 2005;15:1705–1712.
55. Kapadia SB. Multiple myeloma: a clinicopathologic study of 62 consecutively autopsied cases. Medicine (Baltimore) 1980;59:380–392.
56. Oshima K, Kanda Y, Nannya Y, et al. Clinical and pathologic findings in 52 consecutively autopsied cases with multiple myeloma. Am J Hematol 2001; 67:1–5.
57. Sered S, Nikolaidis P. CT findings of perirenal plasmacytoma. AJR Am J Roentgenol 2003;181: 888.
58. Patlas M, Khalili K, Dill-Macky MJ, Wilson SR. Spectrum of imaging findings in abdominal extraosseous myeloma. AJR Am J Roentgenol 2004; 183:929–932.
59. Eble JN. Angiomyolipoma of kidney. Semin Diagn Pathol 1998;15:21–40.
60. Hornick JL, Fletcher CD. PEComa: what do we know so far? Histopathology 2006;48:75–82.
61. Obara W, Sato K, Owari Y, et al. Perinephric angiomyolipoma: a unique development pattern surrounding the kidney. Int J Urol 2005;12:305–307.
62. Prasad SR, Sahani DV, Mino-Kenudson M, et al. Neoplasms of the perivascular epithelioid cell involving the abdomen and the pelvis: cross-sectional imaging findings. J Comput Assist Tomogr 2007; 31:688–696.
63. Israel GM, Bosniak MA, Slywotzky CM, Rosen RJ. CT differentiation of large exophytic renal angiomyolipomas and perirenal liposarcomas. AJR Am J Roentgenol 2002;179:769–773.
64. Hafron J, Fogarty JD, Hoenig DM, Li M, Berkenblit R, Ghavamian R. Imaging characteristics of minimal fat renal angiomyolipoma with histologic correlations. Urology 2005;66:1155–1159.
65. Song T, Shen J, Liang BL, Mai WW, Li Y, Guo HC. Retroperitoneal liposarcoma: MR characteristics and pathological correlative analysis. Abdom Imaging 2007;32:668–674.
66. Chouairy CJ, Abdul-Karim FW, MacLennan GT. Retroperitoneal liposarcoma. J Urol 2007;177: 1145.
67. Kim T, Murakami T, Oi H, et al. CT and MR imaging of abdominal liposarcoma. AJR Am J Roentgenol 1996;166:829–833.
68. Ablett MJ, Vosylius P. Perirenal extramedullary haematopoeisis in myelofibrosis demonstrated on computed tomography. Br J Haematol 2004;124: 406.
69. O'Malley DP. Benign extramedullary myeloid proliferations. Mod Pathol 2007;20:405–415.
70. Georgiades CS, Neyman EG, Francis IR, Sneider MB, Fishman EK. Typical and atypical presentations of extramedullary hemopoiesis. AJR Am J Roentgenol 2002;179:1239–1243.
71. Mesurolle B, Sayag E, Meingan P, Lasser P, Duvillard P, Vanel D. Retroperitoneal extramedullary hematopoiesis: sonographic, CT, and MR imaging appearance. AJR Am J Roentgenol 1996;167: 1139–1140.
72. Kumar M, Duerinckx AJ. Bilateral extraadrenal perirenal myelolipomas: an imaging challenge. AJR Am J Roentgenol 2004;183:833–836.
73. Rao P, Kenney PJ, Wagner BJ, Davidson AJ. Imaging and pathologic features of myelolipoma. RadioGraphics 1997;17:1373–1385.
74. Wagner JR, Kleiner DE, Walther MM, Linehan WM. Perirenal myelolipoma. Urology 1997;49: 128–130.
75. Kenney PJ, Wagner BJ, Rao P, Heffess CS. Myelolipoma: CT and pathologic features. Radiology 1998;208:87–95.
76. Kammen BF, Elder DE, Fraker DL, Siegelman ES. Extraadrenal myelolipoma: MR imaging findings. AJR Am J Roentgenol 1998;171:721–723.

This article meets the criteria for 1.0 credit hour in category 1 of the AMA Physician's Recognition Award. To obtain credit, see accompanying test at http://www.rsna.org/education/rg_cme.html.

Neoplastic and Nonneoplastic Proliferative Disorders of the Perirenal Space: Cross-sectional Imaging Findings

Venkateswar R. Surabhi, MD, et al

RadioGraphics 2008; 28:1005–1017 • **Published online** 10.1148/rg.284075157 • **Content Codes:** GU OI

Page 1013
Renal angiomyolipoma with perinephric extension is the most common macroscopic fat--containing mass in the perirenal region.

Page 1013
The presence of a well-defined renal parenchymal defect and intralesional aneurysms are suggestive of a diagnosis of angiomyolipoma of the kidney rather than a liposarcoma

Page 1012
Perirenal involvement in Erdheim-Chester disease characteristically is manifested as rindlike soft-tissue lesions surrounding the kidneys and ureters.

Page 1009
Imaging features of renal or perinrenal hemangiomas are variable. The depiction of a soft-tissue mass with phleboliths, high signal intensity on T2-weighted images, and delayed or persistent contrast enhancement is suggestive of the diagnosis.

Page 1012
Lung cancer shows a specific predilection for perirenal spread secondary to connections between the perirenal and mediastinal lymphatic vessels.